

## A MULTI-WAVELENGTH STUDY OF PAH-SELECTED STARBURST GALAXIES

T. TAKAGI<sup>1</sup>, H. MATSUHARA<sup>1</sup>, T. WADA<sup>1</sup>, Y. OHYAMA<sup>2</sup>, AND S. OYABU<sup>3</sup>

<sup>1</sup>Institute of Space and Astronautical Science, JAXA, Sagami-hara, Kanagawa 229-8510, Japan

<sup>2</sup>Academia Sinica, Institute of Astronomy and Astrophysics, Taiwan

<sup>3</sup>Graduate School of Science, Nagoya University, Furo-cho, Chikusa-ku, Nagoya, Aichi 464-8602, Japan

*E-mail: takagi@ir.isas.jaxa.jp*

*(Received July 03, 2012; Accepted August, 12, 2012)*

### ABSTRACT

Using extensive mid-IR datasets from AKARI, i.e. 9-band photometry covering the wavelength range from  $2\ \mu\text{m}$  to  $24\ \mu\text{m}$  and the unbiased spectroscopic survey for sources with  $S_{\nu}(9\ \mu\text{m}) > 0.3\ \text{mJy}$ , we study starburst galaxies specifically at the redshift of  $z \sim 0.5$ , whose mid-IR spectra are clearly dominated by the PAH emission features. PAH-selected galaxies, selected with extremely red mid-IR colour due to PAHs, have high rest-frame PAH-to-stellar luminosity ratios, comparable to those in the most active regions in nearby starburst galaxies. Thus, they seem to have active starburst regions spreading over the whole body. Furthermore, some of PAH-selected galaxies are found to have peculiar rest-frame 11-to- $8\ \mu\text{m}$  flux ratios, which is systematically smaller than nearby starburst/AGN spectral templates. This may indicate a systematic difference in the physical condition of ISM between nearby and distant starburst galaxies.

*Key words:* infrared: galaxies; galaxies: starburst; ISM: evolution; dust

### 1. INTRODUCTION

Mid-infrared (IR) surveys are a powerful tool for studying the infrared luminosity function as a function of redshift, an important measure of the cosmic star formation history of the universe (e.g. Goto et al., 2010). However, the empirical estimate of the star formation rate from the mid-IR luminosity suffers uncertainty from the assumption on the mid-IR spectral energy distributions (SEDs), which are usually dominated by the emission from very small grains and PAHs. In many IR extragalactic surveys, PAHs are the only dust species detectable in most of distant galaxies, because of relatively good sensitivity in the mid-IR range. Thus, a better understanding of the mid-IR spectral features, such as the PAH emission, is vital for the study of star formation activity in the distant universe.

### 2. NEP SURVEY

Along with the all-sky survey, AKARI performed 5,088 pointed observations in selected areas of sky during its cold phase with liquid helium. Using 13% of these pointed-observation opportunities, we conducted extragalactic surveys around the North Ecliptic Pole (NEP). A salient characteristics of this survey is its comprehensive mid-IR wavelength coverage, using 9 photometric bands to span the wavelength range from 2 to  $24\ \mu\text{m}$ . Furthermore, we utilized a slit-less spectroscopic capability of the IRC onboard AKARI for an unbiased spectroscopic survey in the mid-IR wavelengths.

#### 2.1. Photometric Survey (NEP-Deep)

The NEP survey is two-tiered, consisting of the NEP-Deep and NEP-Wide surveys with the circular area of  $0.6\ \text{deg}^2$  and  $5.8\ \text{deg}^2$ , respectively. The field configuration of the NEP-Deep survey is shown in Figure 1. Here we mainly use the data from the NEP-Deep survey

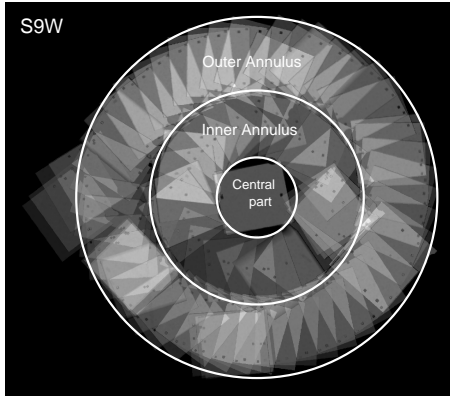


**Fig. 1.** Coverage map of the NEP-Deep survey at  $9\ \mu\text{m}$ . Square patterns indicate the field-of-view of the MIR-S channel of the IRC, each covering  $10' \times 10'$ .

which has follow-up observations over the whole electromagnetic spectrum from X-ray to radio. Detailed descriptions of the NEP-Deep survey and the mid-IR source catalogue are found in Wada et al. (2008) and Takagi et al. (2012), respectively.

### 2.2. Slit-less spectroscopic survey of galaxies (SPICY)

In the SPICY program, we obtained  $5 - 15\ \mu\text{m}$  spectra of mid-IR sources which are flux-limited sample with  $S_\nu(9\ \mu\text{m}) > 0.3\ \text{mJy}$ . The SPICY fields are patchily distributed around the NEP-Deep field, covering  $\sim 1,000\ \text{arcmin}^2$  in total. Most of the SPICY fields lie inside the NEP-Deep field. The spectral resolution of the IRC slit-less spectroscopy is  $R \simeq 50$  and therefore the narrow fine-structure lines, if any, would be smoothed out. The PAH 6.2, 7.7, and  $8.6\ \mu\text{m}$  were simultaneously fitted along with the continuum. From these PAH features, we measured the PAH luminosity as well as the redshift for more than 50 galaxies at  $z < 0.5$ . The PAH luminosity [ $\nu L_\nu(7.7\ \mu\text{m})$ ] is found to be  $10^9 - 10^{11}\ L_\odot$ . The SPICY project and spectral analyses will be presented elsewhere (Ohyama et al., in prep).

### 3. PAH-SELECTED GALAXIES

The excellent mid-IR wavelength coverage of the NEP survey enables us to photometrically identify galaxies whose mid-IR emission is clearly dominated by PAHs. Takagi et al. (2007) demonstrated that the AKARI/IRC all-band photometry is capable of identi-

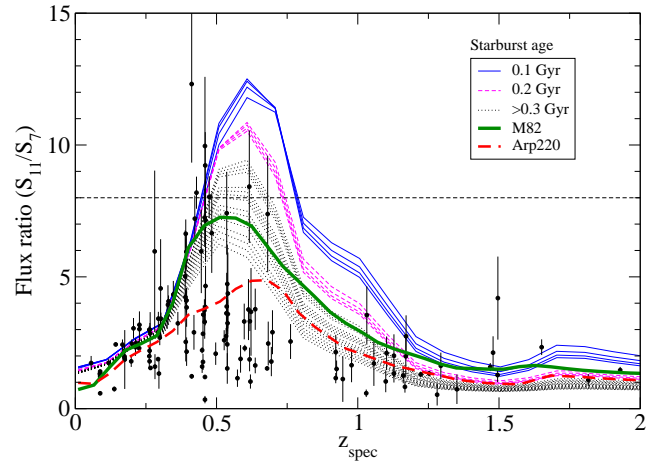


**Fig. 2.** Flux ratio of 11 to  $7\ \mu\text{m}$  as a function of redshift. Expected flux ratios from Arp220 and M82 are depicted as thick dashed and solid lines, respectively. A starburst SED model of Takago et al. (2003) is used for other lines. Horizontal lines indicate the flux ratio of 8, a selection criterion of PAH-selected galaxies. All-band-detected sources with spectroscopic redshift are indicated with solid circles.

fying the approximate spectral shape of the PAH emission, specifically the steep rise in flux at the blue side of the PAH  $6.2\ \mu\text{m}$  feature. Based on this fact, we selected PAH-dominated galaxies at  $z \sim 0.5$  using a single colour, i.e. the 11-to- $7\ \mu\text{m}$  flux ratio as shown in Figure 2. This flux ratio corresponds to the PAH-to-stellar luminosity ratio for galaxies at  $z \sim 0.5$ . We call galaxies with this flux ratio greater than 8 as PAH-selected galaxies. These galaxies are expected to have high specific star formation rate (SFR). Using a longer wavelength filters, such as  $9$  and  $15\ \mu\text{m}$  bands, PAH-selected galaxies at  $z \sim 1$  can be identified (Takagi et al., 2010).

For local galaxies, such high PAH-to-stellar luminosity ratios are found only in intensive star-forming regions (e.g. Wang et al., 2004). For PAH-selected galaxies, we found high PAH-to-stellar luminosity ratios in global measurements. As is found in some of local luminous infrared galaxies, a small region could dominate the total infrared luminosity (e.g. Inami et al., 2010). Even in such extreme cases, PAH-to-stellar luminosity ratio of a galaxy as a whole cannot be as high as  $\sim 10$ , owing to the contribution of stellar luminosity from the other quiescent regions. PAH-selected galaxies seem to be dominated by starburst components with a large

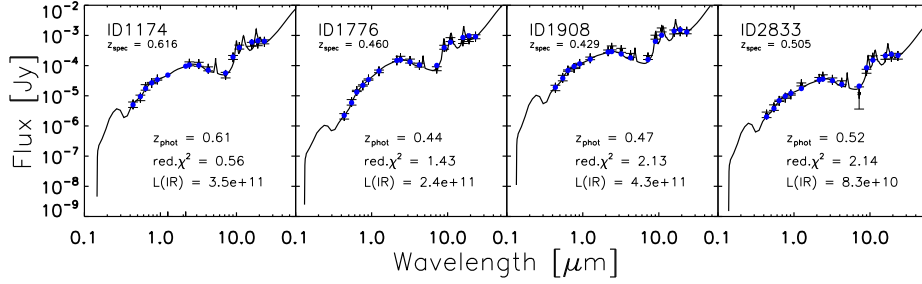


**Fig. 3.** Example of the SED fitting with SBURT. Filled circles and data with error bars indicate the model fluxes with filter convolution and the observed fluxes, respectively.

specific SFR, spreading over the whole body.

#### 4. SED FITTING

We analysed the SED of PAH-selected galaxies using an evolutionary SED model of starburst galaxies (SBURT; Takagi et al., 2003), and also with spectral templates of local galaxies. SBURT is a radiative transfer model of the spherical starburst region, which has centrally concentrated stars and uniformly distributed dust clouds. Fitting parameters are the starburst age, total mass of the system, the compactness of the starburst region (controlling the optical depth), and the type of the extinction curve (MW, LMC, or SMC). In Figure 3, we show the example of the best-fitting SED models for optical-NIR and AKARI/IRC all-band photometries. PAH-selected galaxies are all fitted with the dust model of the MW, which has the highest PAH fraction in dust, i.e. 5%.

We found that SBURT can provide acceptable models for the half of PAH-selected galaxies based on the  $\chi^2$  values. For the rest half of the sample, we show the ratio of the observed to model fluxes as a function of the rest-frame wavelength in Figure 4. These flux ratios indicate that the fit is rather good, except for the 5–7  $\mu\text{m}$  wavelength range where the most prominent PAH features are found. A similar trend can be seen for the good fit sample as well, although it is less significant. Figure 4 shows that the model reproduces the rest-frame 11–15  $\mu\text{m}$  fluxes well, and indicates a large anomaly in the rest-frame 11-to-8  $\mu\text{m}$  flux ratio, i.e. the flux ratio of C-H to C-C mode emission of PAHs. A possible origin of this deviation is the ionization state of PAHs, which affect the absorption cross section of

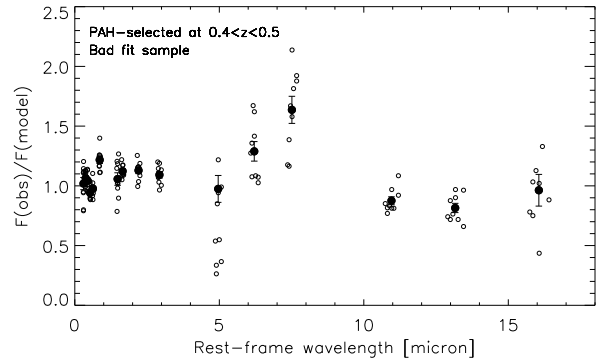


**Fig. 4.** The ratio of the observed to model fluxes of PAH-selected galaxies at  $0.4 < z < 0.5$  as a function of the rest-frame wavelengths. The circles with error bars indicate the average flux ratios.

PAHs specifically around 8  $\mu\text{m}$  (Li & Draine, 2001).

#### 5. PAH INTERBAND FLUX RATIO

The SED fitting analyses indicate a systematic variation of the PAH features, compared to the local template of the PAH features. From the SPICY dataset, we measured the inter-band flux ratio of PAH 6.2-to-7.7  $\mu\text{m}$  and found that this ratio is similar to the values of nearby starburst galaxies. Unfortunately, the wavelength coverage of the SPICY is not wide enough to cover the PAH 11.3  $\mu\text{m}$ . However, the excellent wavelength coverage of photometric data allows us to estimate the PAH luminosity without a significant  $k$ -correction, specifically at 7.7  $\mu\text{m}$ . With the SPICY data, we confirmed that photometrically measured PAH 7.7  $\mu\text{m}$  luminosities linearly correlate with

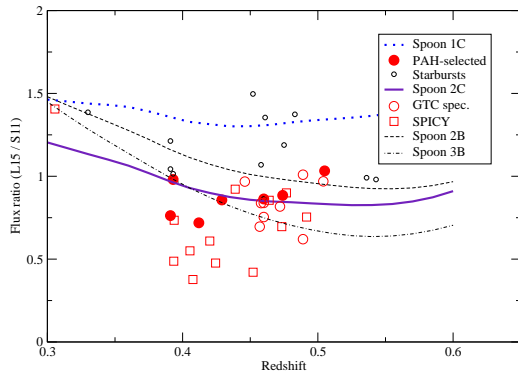


**Fig. 5.** The 15-to-11  $\mu\text{m}$  flux ratio of PAH-selected galaxies at  $z_{\text{spec}} \sim 0.4$ . This flux ratio corresponds to 11-to-8  $\mu\text{m}$  flux ratio at  $z = 0.4$ . Solid lines indicate the flux ratios expected from nearby starburst galaxies/AGNs taken from Spoon et al. (2007).

the spectroscopic measurements.

We investigated the rest-frame 11-to-8  $\mu\text{m}$  flux ratio of PAH-selected galaxies at  $z \simeq 0.4 - 0.5$ , for which the spectroscopic redshift is available. At this redshift, the rest-frame 11-to-8  $\mu\text{m}$  flux ratio can be measured with the AKARI 15-to-11  $\mu\text{m}$  flux ratio. In Figure 5, we compare these flux ratios with those expected from a spectral template of Spoon et al. (2007) which has spectra with a wide variety of the PAH equivalent width and the silicate absorption. We found that the observed flux ratios of PAH-selected galaxies are too small to be reproduced by the nearby spectral template. In a resolved IRC image of M82 (Arimatsu et al., in prep), similar anomaly of the inter-band flux ratio can be found only in small spots around the centre. In PAH-selected galaxies, such anomaly is found for global measurements, indicating the systematic difference in the physical condition of ISM between nearby and distant starburst galaxies.

## ACKNOWLEDGEMENTS

This research is based on observations with AKARI, a JAXA project with the participation of ESA. We would like to thank the AKARI team members for their extensive efforts.

## REFERENCES

- Goto, T., Takagi, T., Matsuhara, H., et al., 2010, Evolution of Infrared Luminosity Functions of Galaxies in the AKARI NEP-Deep Field. Revealing the Cosmic Star Formation History Hidden by Dust, *A&A*, 514, A6+
- Inami, H., Armus, L., Surace, J. A., et al., 2010, The Buried Starburst in the Interacting Galaxy II Zw 096 as Revealed by the Spitzer Space Telescope, *AJ*, 140, 63
- Li, A. & Draine, B. T., 2001, Infrared Emission from Interstellar Dust. II. The Diffuse Interstellar Medium, *ApJ*, 554, 778
- Spoon, H. W. W., Marshall, J. A., Houck, J. R., et al., 2007, Mid-Infrared Galaxy Classification Based on Silicate Obscuration and PAH Equivalent Width, *ApJ*, 654, L49
- Takagi, T., Arimoto, N., Hanami, H., 2003, Evolutionary Spectral Energy Distribution Diagnostics of Starburst Galaxies: Signature of Bimodality, *MNRAS*, 340, 813
- Takagi, T., Matsuhara, H., Goto, T., et al., 2012, The AKARI NEP-Deep Survey: a Mid-Infrared Source Catalogue, *A&A*, 537, A24
- Takagi, T., Matsuhara, H., Wada, T., et al., 2007, Multi-Wavelength Analysis of 18  $\mu\text{m}$ -Selected Galaxies in the AKARI/Infrared-Camera Monitor Field Towards the North Ecliptic Pole, *PASJ*, 59, 557
- Takagi, T., Ohyama, Y., Goto, T., et al., 2010, Polycyclic Aromatic Hydrocarbon (PAH) Luminous Galaxies at  $z \sim 1$ , *A&A*, 514, A5+
- Wada, T., Matsuhara, H., Oyabu, S., et al., 2008, AKARI/IRC Deep Survey in the North Ecliptic Pole Region, *PASJ*, 60, 517
- Wang, Z., Fazio, G. G., Ashby, M. L. N., et al., 2004, The Off-Nuclear Starbursts in NGC 4038/4039 (The Antennae Galaxies), *ApJS*, 154, 193